AFOSR-TR- 79-0199

LEVEL II

PSI TR-158

BISTABLE NOSETIP FLOW STUDIES
INTERIM SCIENTIFIC REPORT

ANALYSIS OF ROUGH WALL TURBULENT HEATING WITH APPLICATION TO BLUNTED FLIGHT VEHICLES

JANUARY 1979

by

M.L. FINSON and P.K.S. WU

Jointly Sponsored by

The Space and Missile Systems Organization
and
The Air Force Office of Scientific Research (AFSC)

Contract F49620-78-C-0028

PHYSICAL SCIENCES INC.
30 COMMERCE WAY, WOBURN, MASS. 01801

Qualified requestors may obtain additional copies from the Defense Documentation Center, all others should apply to the National Technical Information Service.

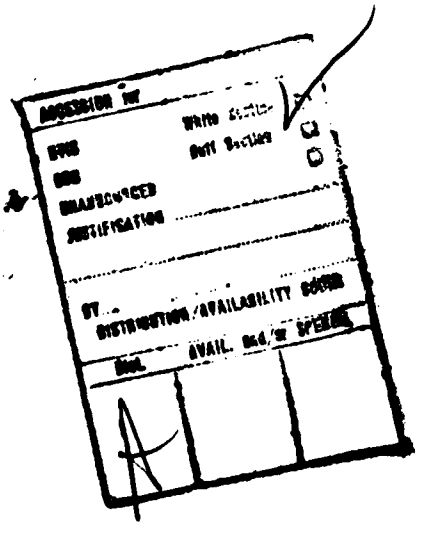

AIR FORCE OFFICE OF SCIENTIFIC RESEARCH (AFSC)
NOTICE OF TRANSMITTAL TO DDC
This technical report has been reviewed and is approved for public release IAW AFR 190-12 (7b).
Distribution is unlimited.
A. D. BLOSE
Technical Information Officer

UNCLASSIFIED
SECURITY CLASSIFICATION OF THIS PAGE (When Data Entered)

REPORT DOCUMENTATION PAGE	READ INSTRUCTIONS BEFORE COMPLETING FORM
1. REPORT NUMBER: AFOSR-TR-79-0199	2. GOVT ACCESSION NO. / 3. RECIPIENT'S CATALOG NUMBER
4. TITLE (and Subtitle): ANALYSIS OF ROUGH WALL TURBULENT HEATING WITH APPLICATION TO BLUNTED FLIGHT VEHICLES	5. TYPE OF REPORT & PERIOD COVERED: INTERIM, 1 Dec 77 - 30 Sep 78 / 6. PERFORMING ORG. REPORT NUMBER
7. AUTHOR(s): M. L. FINSON, P. K. S. WU	8. CONTRACT OR GRANT NUMBER(s): F49620-78-C-0028
9. PERFORMING ORGANIZATION NAME AND ADDRESS: PHYSICAL SCIENCES INC, 30 COMMERCE WAY, WOBURN, MA 01801	10. PROGRAM ELEMENT, PROJECT, TASK AREA & WORK UNIT NUMBERS: 2307A1, 61102F
11. CONTROLLING OFFICE NAME AND ADDRESS: AIR FORCE OFFICE OF SCIENTIFIC RESEARCH/NA, BLDG 410, BOLLING AIR FORCE BASE, D C 20332	12. REPORT DATE: Jan 79 / 13. NUMBER OF PAGES: 35
14. MONITORING AGENCY NAME & ADDRESS (if different from Controlling Office)	15. SECURITY CLASS. (of this report): UNCLASSIFIED / 15a. DECLASSIFICATION DOWNGRADING SCHEDULE

16. DISTRIBUTION STATEMENT (of this Report)

Approved for public release; distribution unlimited.

17. DISTRIBUTION STATEMENT (of the abstract entered in Block 20, if different from Report)

18. SUPPLEMENTARY NOTES

19. KEY WORDS (Continue on reverse side if necessary and identify by block number)
TURBULENT BOUNDARY LAYERS
TURBULENT HEAT TRANSFER
REENTRY HEATING

20. ABSTRACT (Continue on reverse side if necessary and identify by block number)
The effect of surface roughness on turbulent heating rates is studied, using a second-order closure model which specifically describes the effect of roughness elements on the boundary layer. Comparisons with detailed measurement from low speed flat plate tests are presented to verify the model. A significant number of successful comparisons have also been made with wind tunnel heat transfer data, mostly for hemispherical noses. The rough wall computations are analyzed to determine the nature of the roughness influence, and to derive improved heat transfer correlations for engineering applications.

DD FORM 1 JAN 73 1473

UNCLASSIFIED
SECURITY CLASSIFICATION OF THIS PAGE (When Data Entered)

ABSTRACT

The effect of surface roughness on turbulent heating rates is studied, using a second-order closure model which specifically describes the effect of roughness elements on the boundary layer. Comparisons with detailed measurements from low speed flat plate tests are presented to verify the model. A significant number of successful comparisons have also been made with wind tunnel heat transfer data, mostly for hemispherical noses. The rough wall computations are analyzed to determine the nature of the roughness influence, and to derive improved heat transfer correlations for engineering applications.

Conditions of Reproduction

ACKNOWLEDGEMENT

This research was sponsored by the Space and Missile Systems Organization and the Air Force Office of Scientific Research (AFSC), United States Air Force, under Contract #F49620-78-C-0028. The United States Government is authorized to reproduce and distribute reprints for governmental purposes notwithstanding any copyright notation hereon.

TABLE OF CONTENTS

LIST OF FIGURES

I. INTRODUCTION

It is well known that surface roughness can cause significant increases in turbulent skin friction and heat transfer. An understanding of roughness effects is essential to accurate design predictions for a wide variety of applications, including ships, aircraft, turbine blades, missiles, and reentry vehicles. The present study was motivated primarily by the last application. At low flight altitudes, the thickness of the boundary layer on the blunted nose region of a hypersonic reentry vehicle can easily be less than the inherent surface roughness of practical heatshield materials, and roughness effects dominate the heat transfer.

Most available models for the influence of surface roughness on boundary layer behavior are essentially extensions of Nikuradse's study of pipes roughened with sand,[1] and the application of Nikuradse's results to flat plates by Prandtl and Schlichting.[2] Dvorak[3] used integral methods in which the skin friction coefficient is specified as a function of boundary layer thickness and roughness height. Using this specification, moment equations are solved for the displacement and momentum thicknesses. Chen[4] extended this approach to predict heat transfer, by using the Stanton number correlation derived from subsonic data by Owen and Thomson.[5] In this approach, the stagnation enthalpy profile was equated to the velocity profile. A similar model has recently been developed for reentry vehicles by Dahm et al.[6] Here again, a momentum integral approach is used, with the skin friction and heat transfer coefficients based on correlations of the low speed flat plate data of Healzer et al.[7] and the Mach 2.9 flat plate measurements of Reda[8] (c_f only). The roughness augmentation of heat transfer was found to be about 60% of the skin friction augmentation, although it was noted that the range of k/θ values covered by the data was somewhat limited.

A somewhat more involved approach was taken by Saffman and Wilcox,[9] utilizing a two-equation turbulence model. However, the effect of

roughness was treated rather empirically, by making the boundary condition for pseudo-vorticity at the wall a function of roughness height. This dependence was derived so as to fit the observed variation of the "law of the wall" velocity deficit with roughness. Some encouraging profiles were also computed for the mean and fluctuating velocities. However, heat transfer was again determined by invoking a Reynolds analogy with the skin friction.

The present study employs a second-order turbulence model with several attractive features. Most importantly, it contains a fundamental description for the effect of roughness elements on the boundary layer. Also, the dependent variables include fluctuating temperatures as well as velocity fluctuations, so that no assumptions have to be introduced relating the heat transfer and skin friction. Finally, solutions are obtained by finite-difference techniques, integrating from the wall ($y = 0$), with no assumptions regarding profiles or behavior in the limit $y \to 0$. Computed results will be compared with a variety of low speed and supersonic data, and the nature of the roughness effect on friction and heat transfer will be described. Suggestions will be advanced for improved engineering specifications.

II. ROUGH WALL TURBULENCE MODEL

The turbulence model used here is one in which closure approximations are applied at the second-order. With the exception of the treatment of roughness (to be discussed in detail below), the formulation is somewhat standard at this time, and has been successfully applied to a variety of smooth wall boundary layer and free shear flows. The model accounts for both mean and fluctuating velocities and temperatures. The dependent velocity variables are the mean velocity vector U_i, the Reynolds stress tensor $\overline{u_i' u_j'}$, and the isotropic dissipation rate $\tilde{\varepsilon}$. Under the boundary layer approximation, this set of variables reduces to U, V, $\overline{u'^2}$, $\overline{v'^2}$, $\overline{w'^2}$, $\overline{u'v'}$, and $\tilde{\varepsilon}$. In practice, it is convenient to replace $\overline{u'^2}$, $\overline{v'^2}$, $\overline{w'^2}$ by the kinetic energy $q^2 \equiv (\overline{u'^2} + \overline{v'^2} + \overline{w'^2})/2$ and two measures of the degree of anisotropy $S_{11} \equiv \overline{u'^2} - 2/3\, q^2$, $S_{22} \equiv \overline{v'^2} - 2/3\, q^2$.

For steady flow, the governing equations include continuity:

$$\frac{\partial}{\partial x_i}(\rho U_i) = 0 \tag{1}$$

the mean momentum equation:

$$\rho U_k \frac{\partial U}{\partial x_k} = -\frac{\partial \bar{p}}{\partial x} - \frac{\partial}{\partial y}(\rho \overline{uv}) + \frac{\partial}{\partial y}\left(\mu \frac{\partial U}{\partial y}\right) - R_u \tag{2}$$

and, for the five second-order quantities:

$$\rho U_k \frac{\partial q^2}{\partial x_k} = -\rho \overline{uv} \frac{\partial U}{\partial y} - \rho \tilde{\varepsilon} + 0.2 \frac{\partial}{\partial y}\left[\rho \frac{q^2 v^2}{\tilde{\varepsilon}} \frac{\partial}{\partial y}(q^2 + v^2)\right]$$

$$+ \frac{\partial}{\partial y} \mu \frac{\partial q^2}{\partial y} + (S_{22} - S_{11}) \rho \frac{\partial U}{\partial x} + R_q \tag{3}$$

$$\rho U_k \frac{\partial S_{11}}{\partial x_k} - \frac{14}{33}\rho\overline{uv}\frac{\partial U}{\partial y} - C_E\rho\frac{\Phi}{q^2}S_{11} + 0.2\frac{\partial}{\partial y}\left[\rho\frac{q^2v^2}{\Phi}\frac{\partial}{\partial y}\left(S_{11} - \frac{2}{3}v^2\right)\right]$$

$$+ \frac{\partial}{\partial y}\mu\frac{\partial S_{11}}{\partial y} - \rho\left[\frac{8}{15}q^2 + \frac{2}{33}S_{11} + \frac{1}{33}S_{22}\right]\frac{\partial U}{\partial x} \qquad (4)$$

$$\rho U_k \frac{\partial S_{22}}{\partial x_k} \frac{13}{33}\rho\overline{uv}\frac{\partial U}{\partial y} - C_E\rho\frac{\Phi}{q^2}S_{22} + 0.2\frac{\partial}{\partial y}\left[\rho\frac{q^2v^2}{\Phi}\frac{\partial}{\partial y}\left(S_{22} - \frac{4}{3}v^2\right)\right]$$

$$+ \frac{\partial}{\partial y}\mu\frac{\partial S_{22}}{\partial y} + \rho\left[\frac{8}{15}q^2 + \frac{1}{33}S_{11} + \frac{2}{33}S_{22}\right]\frac{\partial U}{\partial x} \qquad (5)$$

$$\rho U_k \frac{\partial\overline{uv}}{\partial x_k} - \rho\left[\frac{4}{15}q^2 - \frac{2}{11}S_{11} + \frac{5}{22}S_{22}\right]\frac{\partial U}{\partial y} - C_E\rho\frac{\Phi}{q^2}\overline{uv}$$

$$+ 0.4\frac{\partial}{\partial y}\left[\rho\frac{q^2v^2}{\Phi}\frac{\partial\overline{uv}}{\partial y}\right] + \frac{\partial}{\partial y}\mu\frac{\partial\overline{uv}}{\partial y} \qquad (6)$$

$$\rho U_k \frac{\partial\Phi}{\partial x_k} - 1.25\,\rho\frac{\overline{uv}}{q^2}\frac{\partial U}{\partial y}\Phi - C_\Phi\rho\frac{\Phi^2}{q^2} + 177.6\,\rho\frac{\nu^2q^2}{y^4}$$

$$+ 0.322\frac{\partial}{\partial y}\left[\rho\frac{q^2v^2}{\Phi}\frac{\partial\Phi}{\partial y}\right] + \frac{\partial}{\partial y}\mu\frac{\partial\Phi}{\partial y} - 1.25\,\rho\frac{u^2}{q^2}\frac{\partial U}{\partial x}\Phi + R_\Phi \qquad (7)$$

where $C_E = \dfrac{1.2 + 12.5\,\pi/Re_\Lambda}{1 + 12.5\,\pi/Re_\Lambda}$,

$$C_\Phi = \frac{\left(0.288 + 6.6\,\pi/Re_\Lambda + 35\,\pi^2/Re_\Lambda{}^2\right)}{(0.4 + 5\,\pi/Re_\Lambda)^2}$$

and Re_Λ is the turbulent Reynolds number $q\Lambda/\nu$, with Λ being related to the dissipation rate by

$$\Phi \quad 0.4\frac{q^3}{\Lambda} + 5\pi\nu\frac{q^2}{\Lambda^2} = 0.4\frac{q^3}{\Lambda}(1 + 12.5\pi/Re_\Lambda) \tag{8}$$

The various terms on the right side of Eqs. 3-7 describe, respectively, the processes of production, dissipation, turbulent diffusion, molecular diffusion, and streamwise acceleration. The required closure approximations have been developed from basic laboratory turbulence experiments, wherever possible (see refs. 10-13 for details). We shall not describe the results here, except to note that they are similar to those of Launder et al.[14-16]

For flows with compressibility or heat transfer, the analogous variables involving the temperature (or, more precisely, the static enthalpy h) are required. These consist of the static enthalpy $\bar{h}$, the mean square fluctuating enthalpy $\overline{h'^2}$, and the transverse and axial components of the Reynolds heat flux $\overline{v'h'}$ and $\overline{u'h'}$. Required closure approximations have been made in a manner analogous to those leading to the velocity equations above. The resulting enthalpy equations are:

$$\rho\frac{D\bar{h}}{Dt} \quad \bar{U}_i\frac{\partial\bar{p}}{\partial x_i} - \frac{\partial}{\partial y}(\rho\overline{v'h'}) + \frac{1}{Pr}\frac{\partial}{\partial y}\left(\mu\frac{\partial\bar{h}}{\partial y}\right) + \mu\left(\frac{\partial U}{\partial y}\right)^2 + \rho\Phi \tag{9}$$

$$\rho\frac{D\overline{h'^2}}{Dt} \quad - 2\rho\overline{v'h'}\frac{\partial\bar{h}}{\partial y} - C_{T_1}\rho\frac{\Phi}{q^2}\overline{h'^2} + 0.40\frac{\partial}{\partial y}\left(\rho\frac{q^2v^2}{\Phi}\frac{\partial\overline{h'^2}}{\partial y}\right)$$

$$+ \frac{1}{Pr}\frac{\partial}{\partial y}\left(\mu\frac{\partial\overline{h'^2}}{\partial y}\right) \tag{10}$$

$$\rho\frac{D\overline{v'h'}}{Dt} = -\rho v^2\frac{\partial\bar{h}}{\partial y} - 0.09835\,\bar{\rho}\,\overline{u'h'}\frac{\partial U}{\partial y} - C_{T_2}\rho\frac{\Phi}{q^2}\overline{v'h'}$$

$$+ 0.80\frac{\partial}{\partial y}\left(\rho\frac{q^2v^2}{\Phi}\frac{\partial}{\partial y}\overline{v'h'}\right) + \frac{1}{Pr}\frac{\partial}{\partial y}\left(\mu\frac{\partial\overline{v'h'}}{\partial y}\right) \tag{11}$$

$$\rho \frac{D\overline{u'h'}}{Dt} - 0.3989\, \rho \overline{v'h'} \frac{\partial U}{\partial y} - \rho \overline{uv} \frac{\partial \bar{h}}{\partial y} - C_{\Gamma_2} \rho \frac{\Phi}{q^2} \overline{u'h'}$$

$$+ 0.40 \frac{\partial}{\partial y} \left(\rho \frac{q^2 v^2}{\xi} \frac{\partial \overline{u'h'}}{\partial y} \right) + \frac{1}{Pr} \frac{\partial}{\partial y} \left(\mu \frac{\partial \overline{u'h'}}{\partial y} \right) \qquad (12)$$

where $C_{\Gamma_1} \quad \dfrac{0.8 + 7.5\,\pi/Re_\Lambda}{1 + 12.5\,\pi/Re_\Lambda}$

$C_{\Gamma_2} \quad \dfrac{1.165 + 12.5\,\pi/Re_\Lambda}{1 + 12.5\,\pi/Re_\Lambda}$

It should be noted that terms involving fluctuating densities (ρ') have been dropped in deriving Eqs. (1) - (12). This is generally permissible if the edge Mach number is below 4 or 5, as is usually the case for nosetip regions. However, the dominant effects of density fluctuations can be included by defining a generalized Reynolds stress $R_{ij} = \overline{\rho u_i u_j}/\bar{\rho} = \overline{u_i' u_j'} + \overline{\rho' u_i' u_j'}/\bar{\rho}$. Once this is done, the primary effect of density fluctuations is contained in a relatively unimportant diffusional term involving $\overline{\rho' v'}$, which can be related to $\overline{v'\Gamma'}$. The resulting formulation has yielded good comparisons with the measurements of Horstman et al.[17] in a boundary layer at $M_e \sim 7$.

The terms R_u, R_q, R_Φ contain the effect of roughness on the boundary layer. Only distributed roughness (comparable to sand-grain roughness) is considered here, and we make the fundamental assumption that the flow around individual elements is attached to the elements. For two-dimensional roughness, or closely packed distributed roughness, the flow might be treated more appropriately as cavity flows between the elements. (It must be pointed out that the present approximation, in which the flow approaching an element is assumed to be attached and parallel to the wall even after having flowed past many upstream elements, can be improved upon for many realistic surfaces.)

Roughness elements provide a distributed sink (due to drag) for mean momentum, and distributed sources for kinetic energy and dissipation. We idealize the rough surface as being made up of identical elements (although the extension to a size distribution is feasible), with simple shapes such as cones or hemispheres. The bottom of the elements corresponds to $y = 0$. Let k be the element height, $D(y)$ the element diameter at height y (for $0 \leq y \leq k$), and ℓ be the average center-to-center element spacing. Then, viewing flow around an element at height y as two dimensional, the form drag between $y - \delta y/2$ and $y + \delta y/2$ is

$$\frac{1}{2} \rho U^2 C_D D(y) \delta y$$

To relate this to drag/unit volume, we note that there are ℓ^{-2} elements per unit surface area, so that the appropriate differential volume is $\ell^2 \delta y$ and the sink term for mean momentum is

$$R_u = \frac{1}{2} \rho U^2 C_D D/\ell^2 \tag{13}$$

We could specify $C_D = 1$ for the drag coefficient, appropriate to infinite circular cylinders at local Reynolds numbers above the Stokes flow regime. However, lower values such as 0.5 are more appropriate for finite elements such as cones and hemispheres, and use of such a value provides a first-order correction for the three-dimensional nature of the flow about the elements.

Specification of the source terms R_q and R_ϕ is more speculative, but these terms are generally smaller than the natural production terms and hence less critical to the model. Fluctuations are introduced as disturbances in the wakes of the elements. By analogy with familiar wake flows, fluctuating velocity components should be on the order of two-tenths of the local flow velocity (see, for example, Ref. 18). Thus, the kinetic energy created per unit volume is

$$R_q \quad 0.04\ \rho U^3\ D/\ell^2 \tag{14}$$

A low Reynolds number cutoff to this term was also considered, anticipating that the wakes of elements should be laminar below some minimum value of $\rho UD/\mu$. However, in such situations, the local flow velocity U is sufficiently small that R_q is already negligible.

The role of the source term for dissipation R_Φ is to control the wavelength of the fluctuations created by the roughness elements. Again, by the wake analogy, this wavelength should be comparable to the diameter of the element. Then, following the reasoning leading to Eq. 14,

$$R_\Phi \quad 0.04\ \rho U^3 \nu/(D\ell^2) \tag{15}$$

In evaluating the calculations presented below, this term was found to be negligible. However, the term is given here for the sake of completeness.

The distributed source or sink terms given by Eqs. (13), (14), and (15) are the only ones that need be considered. If oscillations in the wake of an element are approximately isotropic, there should be no significant creation of the anisotropic components $\overline{u'v'}$, $S_{11} \quad \overline{u'^2} - 2/3\,q^2$, $S_{22} \quad \overline{v'^2} - 2/3\,q^2$. Except in the Stokes flow regime, heat transfer to an element should be small. Therefore, there should be no distributed source or sink terms in the equations for the thermal variables.

Boundary conditions to Eqs. (1) - (12) are obvious: fluctuating quantities are zero at a solid wall or at the outer edge (if there is no free-stream turbulence). For numerical solutions, the equations are first transformed to the standard streamfunction coordinate, guaranteeing continuity and eliminating the normal velocity V. The transverse coordinate is also normalized by the edge value of the stream function, so that additional mesh points need not be carried in the free stream to allow for boundary layer growth. For proper resolution of the region near the wall,

a linear mesh in the logarithm of the streamfunction is used. The finite-difference equations are solved with a block tridiagonal Newton-Raphson technique.

III. INCOMPRESSIBLE TURBULENT BOUNDARY LAYERS

The basic case of a low speed boundary layer on a flat plate is important to examine, if only because detailed measurements are available. In particular, the experiments of Moffat and co-workers[7,19,20] on the flow over a plate covered with 0.05 inch diameter spherical balls provide data on skin friction, heat transfer, and profiles of the mean and fluctuating quantities.

Figure 1 compares the results of our model with the mean velocity data, plotted in law-of-the-wall coordinates. Obviously, there is a significant shift in the mean velocity, although the smooth wall and rough wall profiles are more alike when plotted against y/δ. The three components of the kinetic energy are shown in Fig. 2, and Fig. 3 gives the Reynolds stress profile. Perhaps the only discrepancy occurs for the rms velocity component in the flow direction (u') near the wall. However, this effect seems to occur with all second-order models, even on smooth walls. It has yet to be explained properly, but seems not to affect any other boundary layer properties of interest. The roughness effect is apparently substantial in Figs. 2 and 3; much if this could be scaled out by normalizing the fluctuating velocities by the friction velocity u_τ rather than the edge velocity.

Finally, the skin friction coefficient and Stanton number, $\dot{q}/\rho_e u_e (H_e - H_w)$, are shown as a function of downstream distance and flow velocity in Figs. 4 and 5. Increasing the flow velocity leads to a thinner boundary layer and a larger effect of roughness. Although the smooth wall case was not investigated by Healzer et al.[7], the present calculations are in good agreement with classical values. Again, the model agrees well with the data, and it is noted that the effect of roughness on skin friction is greater than that on heat transfer. For the case with the lowest velocity (32 ft/sec), transition was apparently not far upstream of the measured

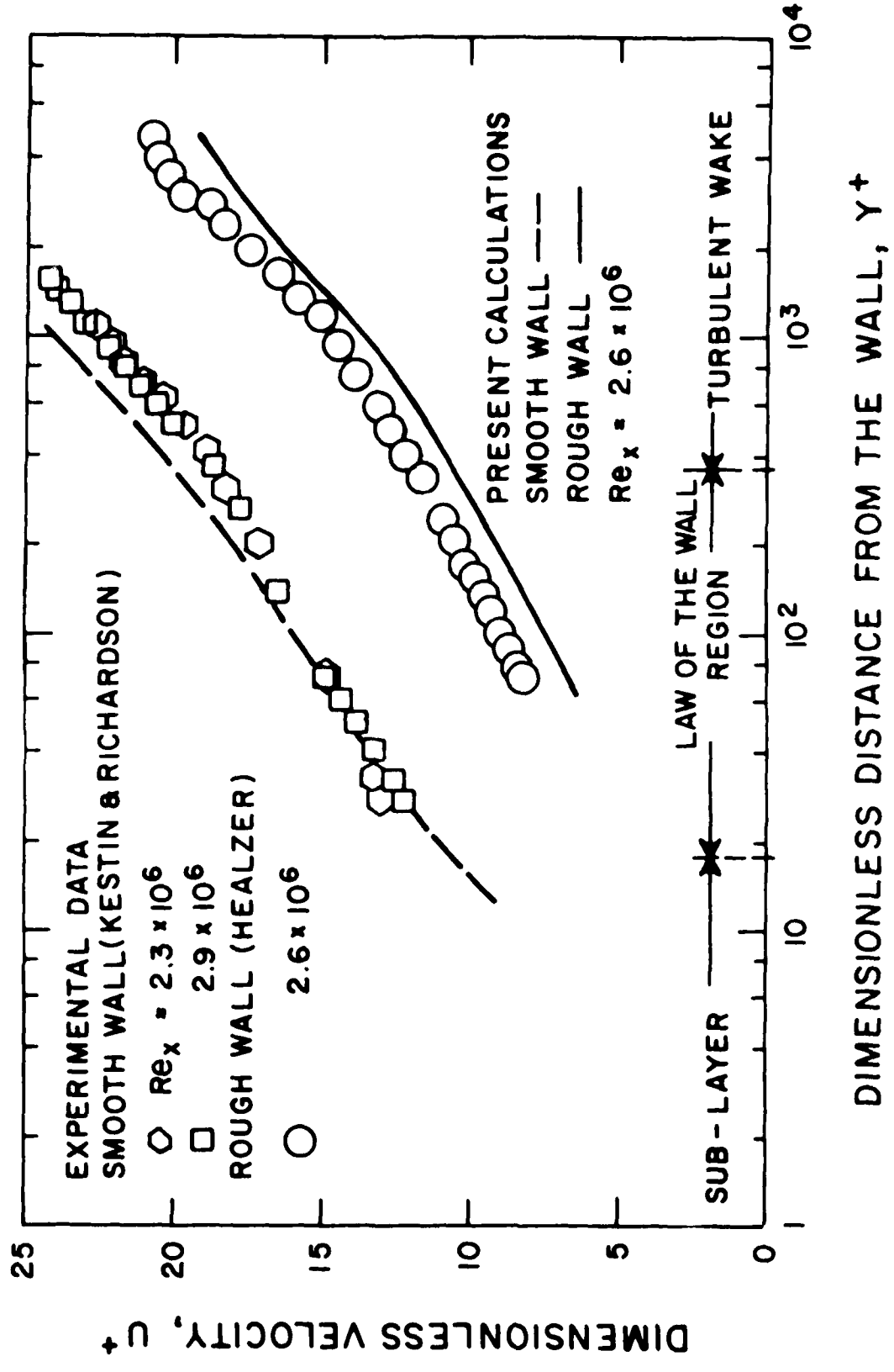

Fig. 1 Flat-Plate Velocity Profiles for Both Rough and Smooth Walls.

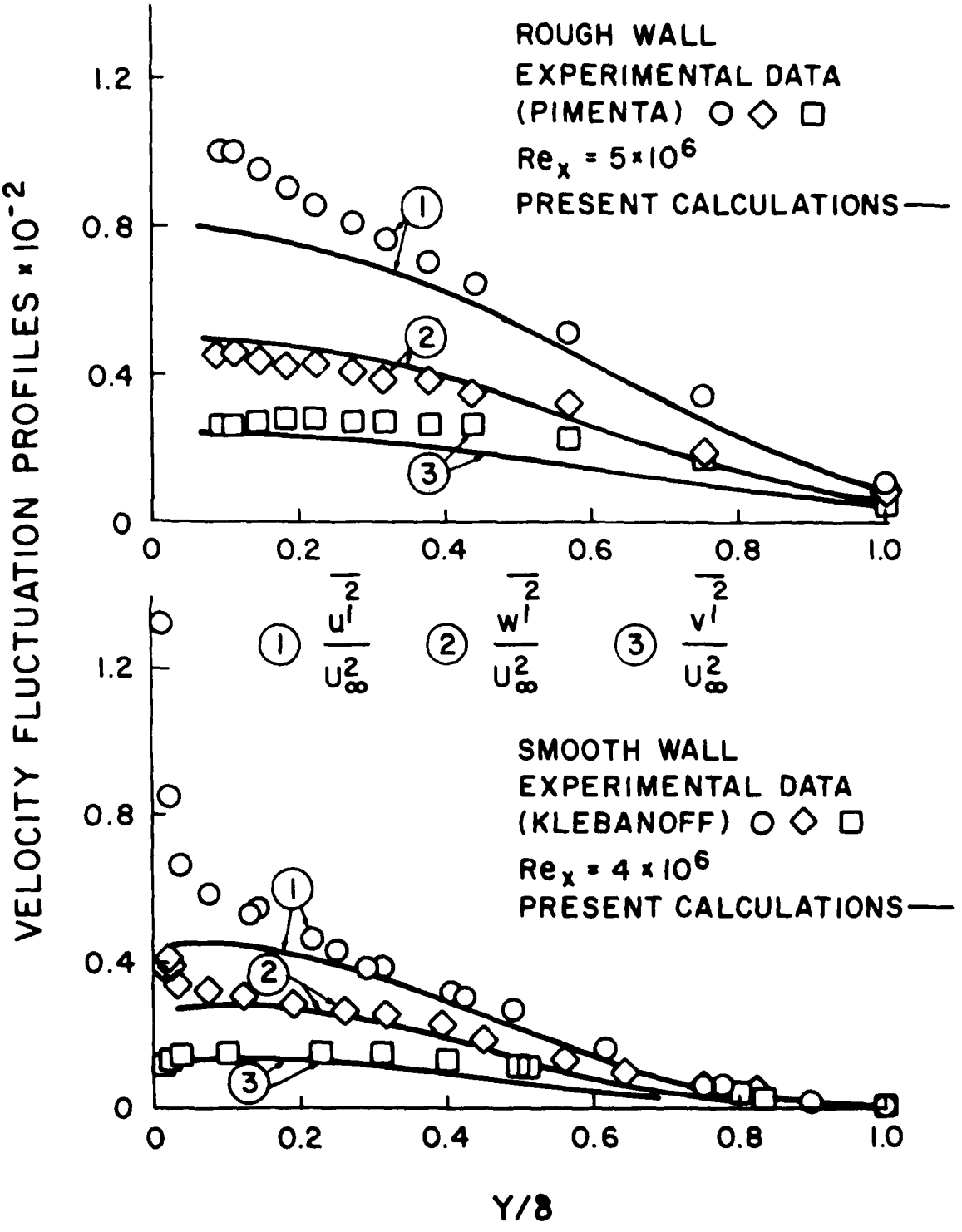

Fig. 2 Velocity Fluctuation Components for Both Rough and Smooth Walls.

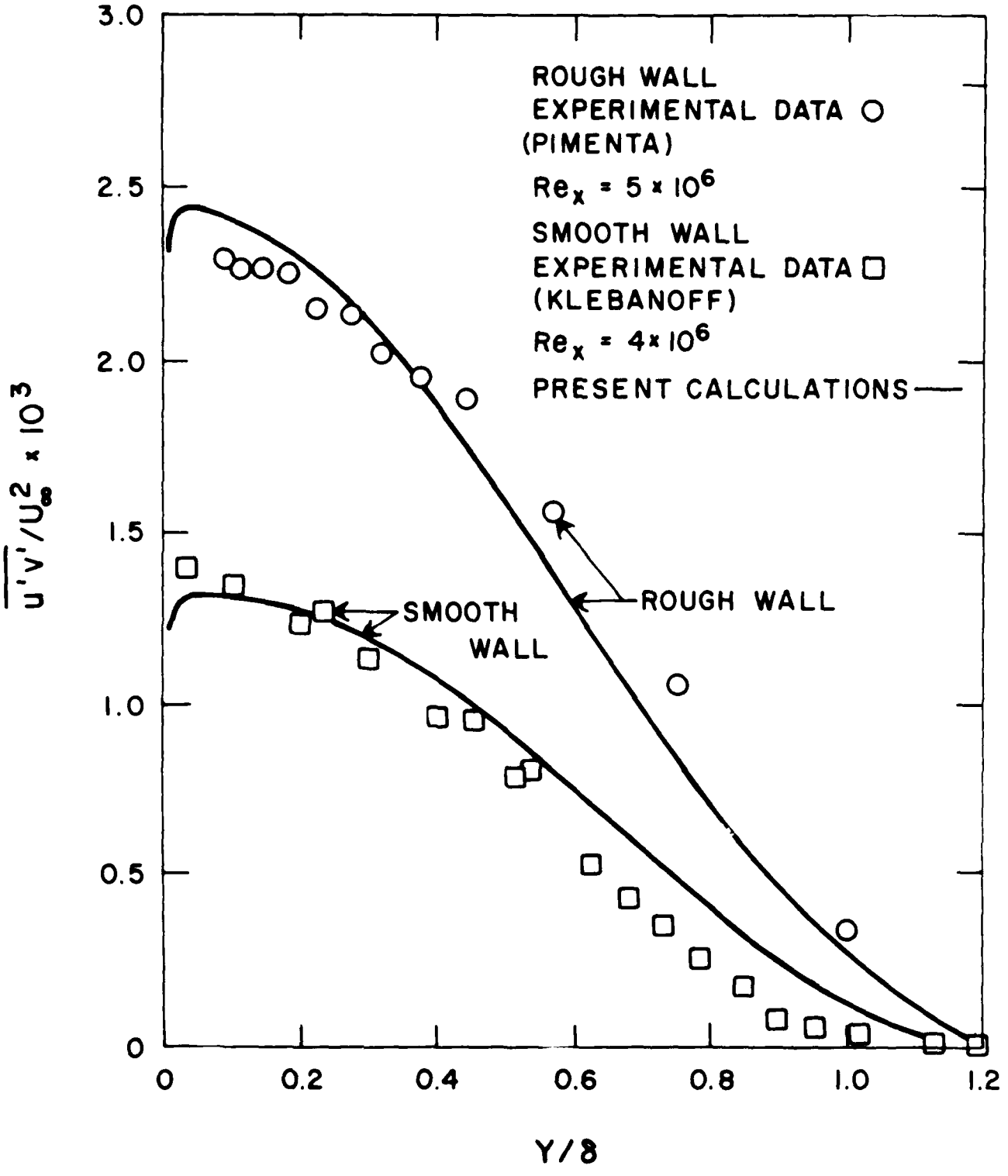

Fig. 3 Profiles of the Reynolds Stress for Both Rough and Smooth Walls.

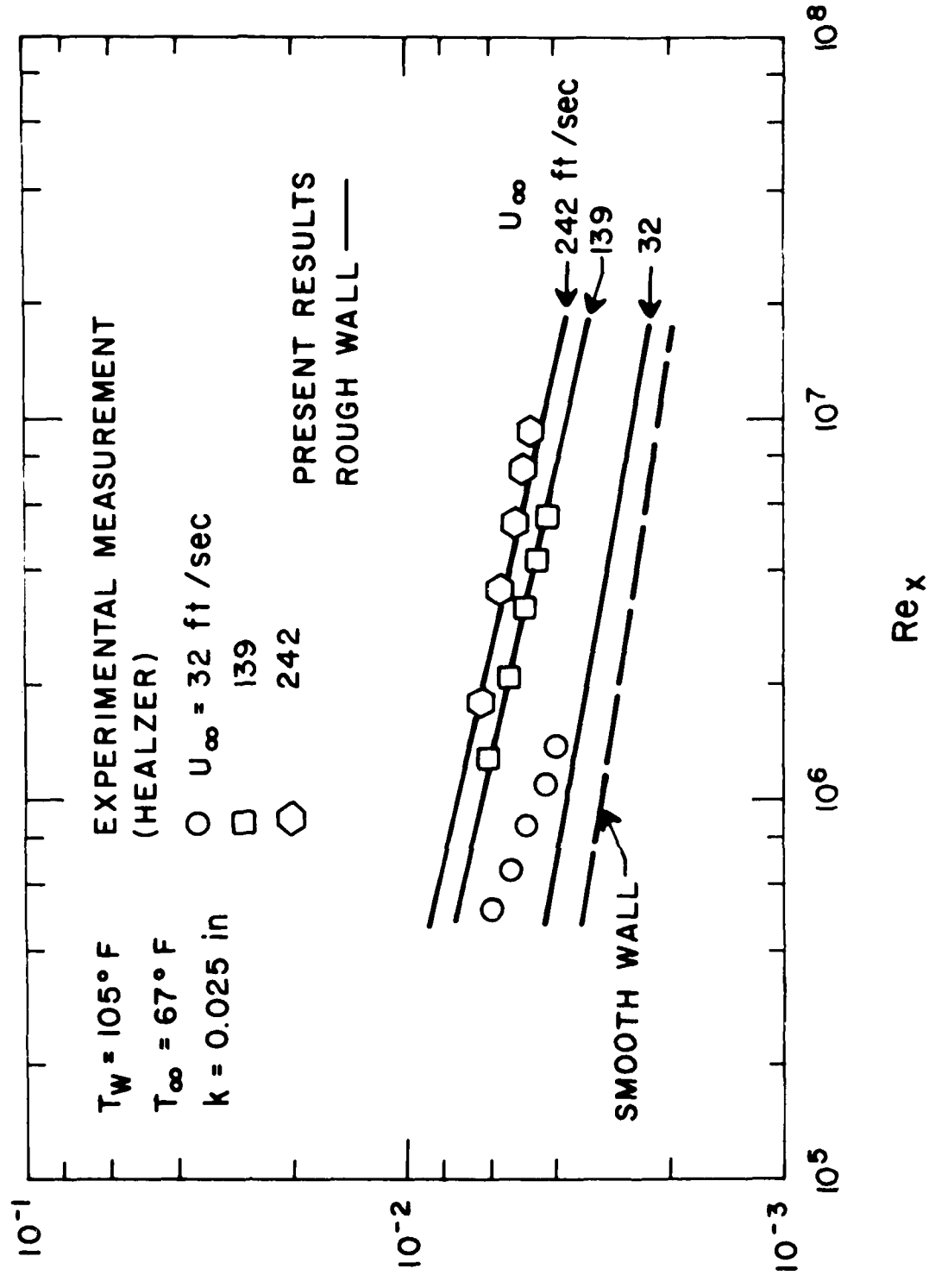

Fig. 4 Skin Friction Coefficient on a Roughened Flat-Plate as Function of Downstream

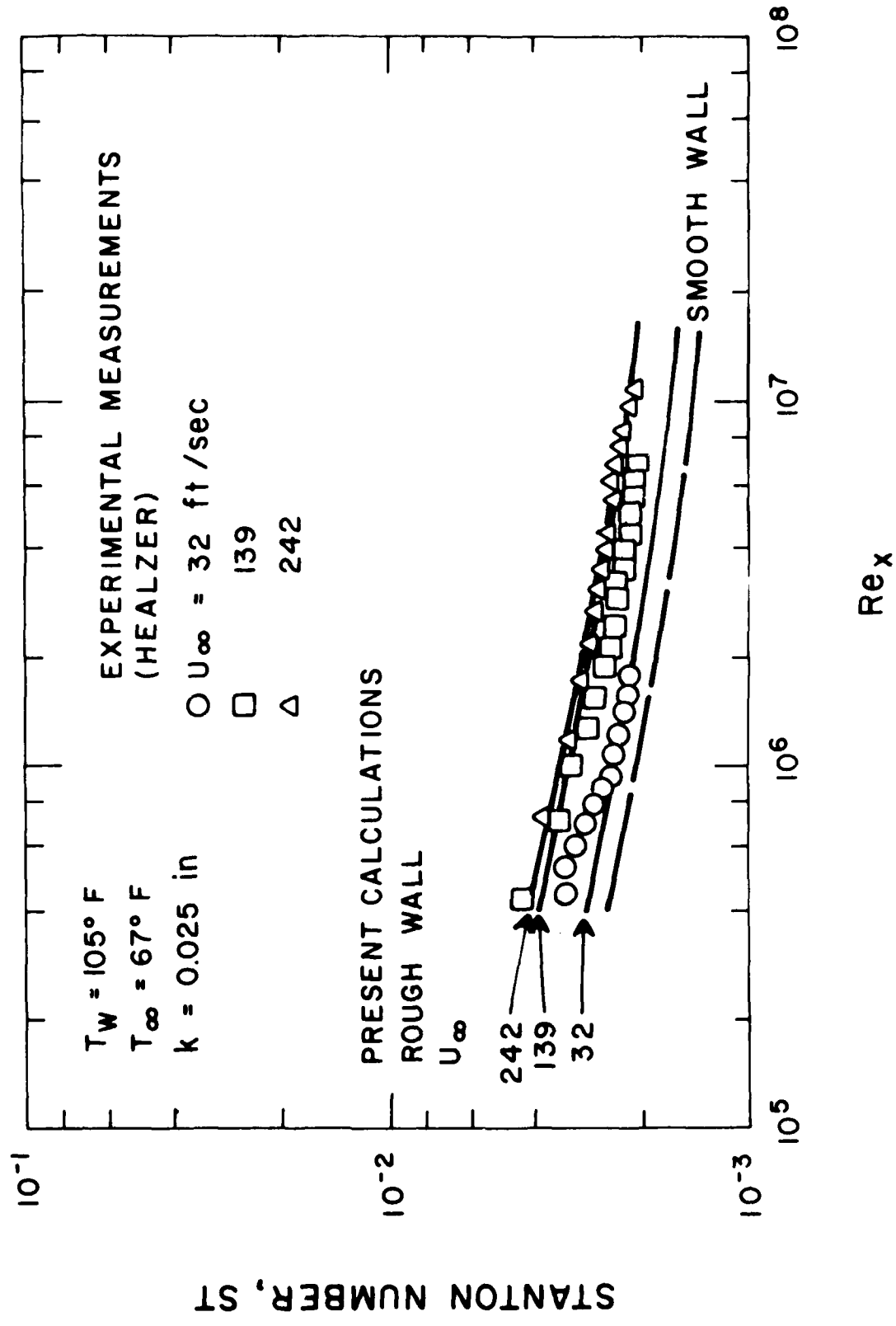

Fig. 5 Normalized Heat Transfer (Stanton Number) Distribution as Function of Downstream Distance

stations and the boundary layer was still approaching the fully-developed turbulent state (the computations were started well upstream, $Re_x \leq 10^4$, and had reached fully-developed behavior).

IV. SUPERSONIC BLUNT NOSE HEAT TRANSFER

Of more practical interest is the heat transfer to the blunted nose region of a high speed flight vehicle. At sufficiently high Reynolds numbers, corresponding to low flight altitudes, the transition location can be quite close to the stagnation point. Also, the boundary layer momentum thickness can be as small as one mil, so that only a highly polished surface would behave in a smooth manner.

The data considered in this section were obtained by the Acurex Corp. under the PANT program,[21] in NSWC Tunnel No. 8 at a freestream Mach number of 5. The thin-wall calorimeter models generally had a nose radius of 2.5 in. Various degrees of surface roughness were generated either by grit blasting or by brazing particles onto the surface; the resulting roughness is thought to be similar in character to sand grain roughness, and the quoted roughness heights are "peak to valley" values (which might be slightly larger than the equivalent sand grain roughness). The ratio of wall temperature to freestream total temperature was in the range 0.4 - 0.7.

Figures 6 through 9 show comparisons with the PANT heat transfer coefficient, $\dot{q}/(T_e - T_w)$, data versus distance from the stagnation point, for decreasing freestream unit Reynolds number. The computations were started near the stagnation point ($S/R_N < 0.01$) with a laminar profile. The effect of roughness generates a turbulent boundary layer relatively quickly, although this procedure should not be considered an accurate prediction of transition. In some cases, such as the smooth case of Fig. 6, the local Reynolds number is insufficient for establishment of a turbulent boundary layer for some distance from the stagnation point ($S/R_N \cong 0.25$ in that case).

It appears from Figs. 6 through 9 that the theory generally provides for good agreement with the measurements. A few points should be made, however: i) the smooth wall case was almost certainly not fully turbulent,

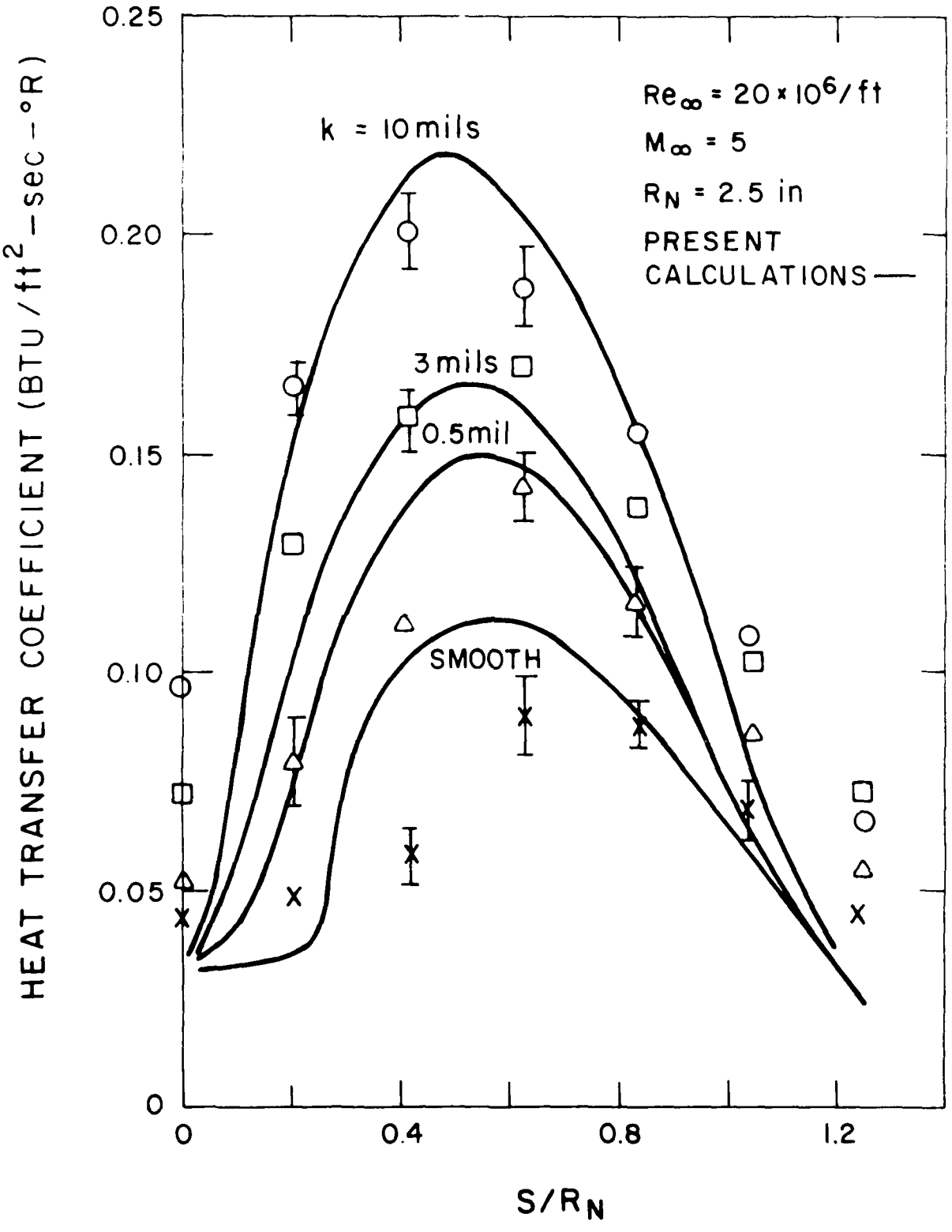

Fig. 6 Comparison With PANT Heat Transfer Data
$Re_\infty = 20 \times 10^6/ft.$

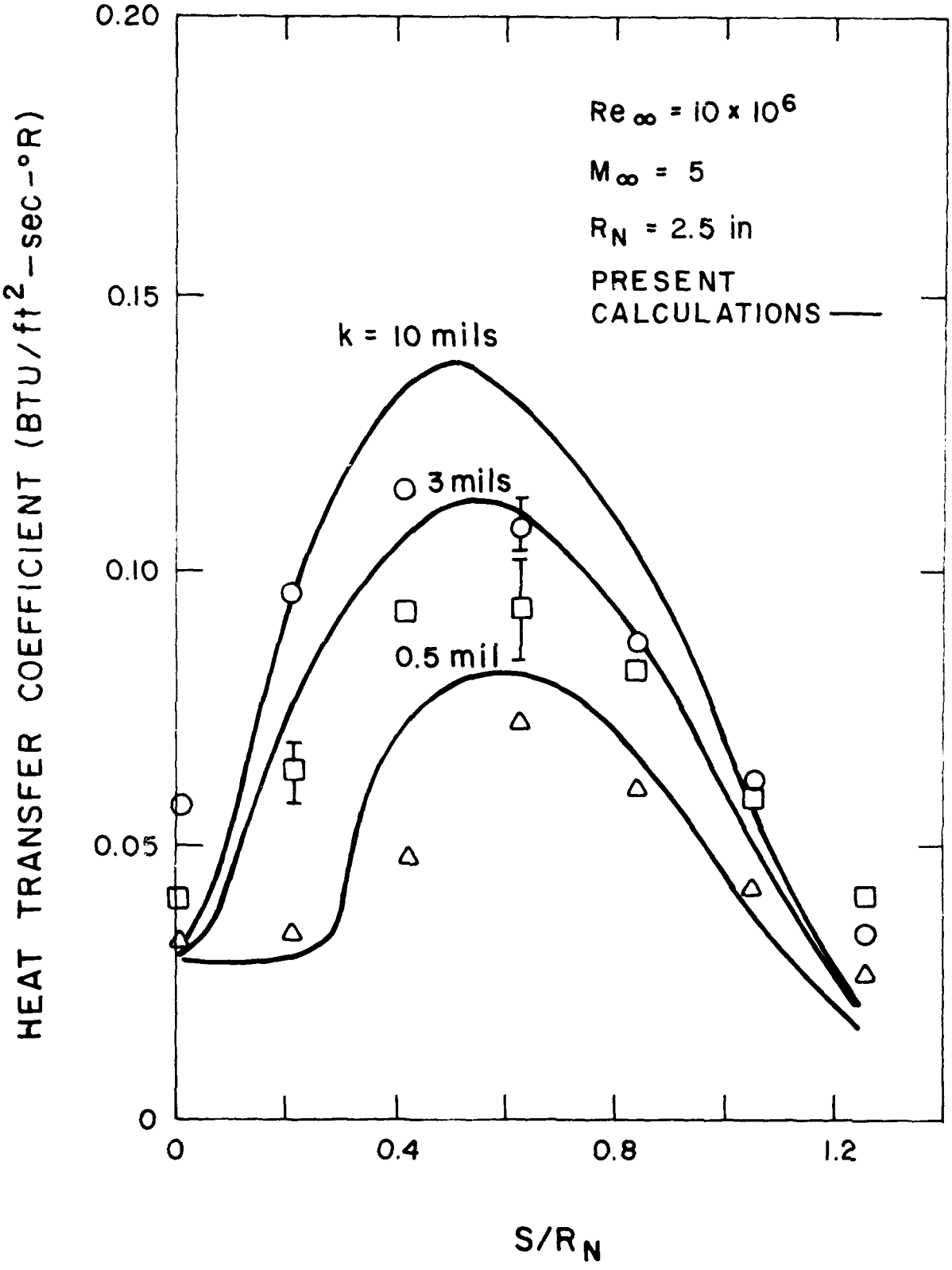

Fig. 7 Comparison With PANT Heat Transfer Data
$Re_\infty = 10 \times 10^6$/ft.

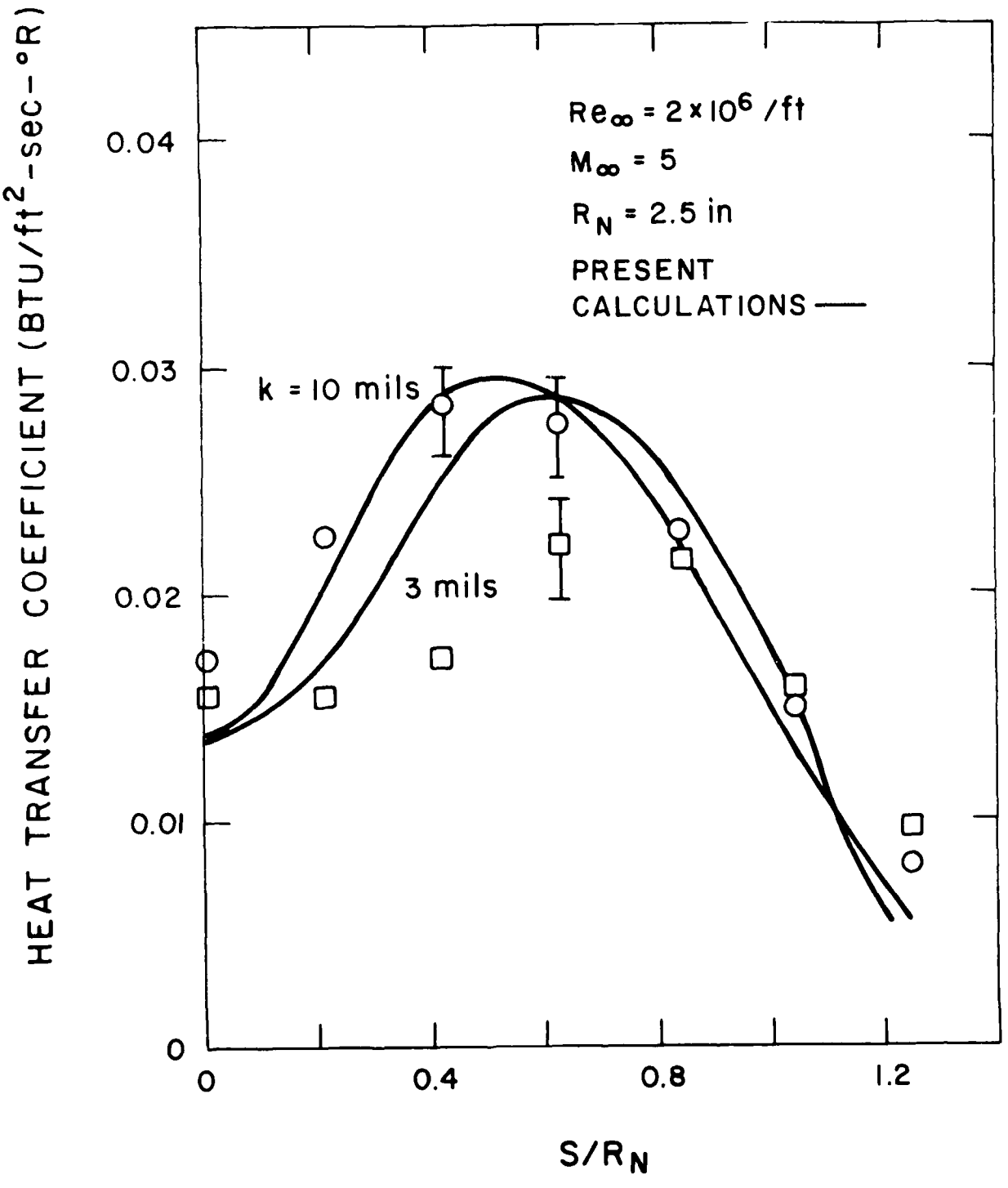

Fig. 8 Comparison With PANT Heat Transfer Data
$Re_\infty = 2 \times 10^6$/ft.

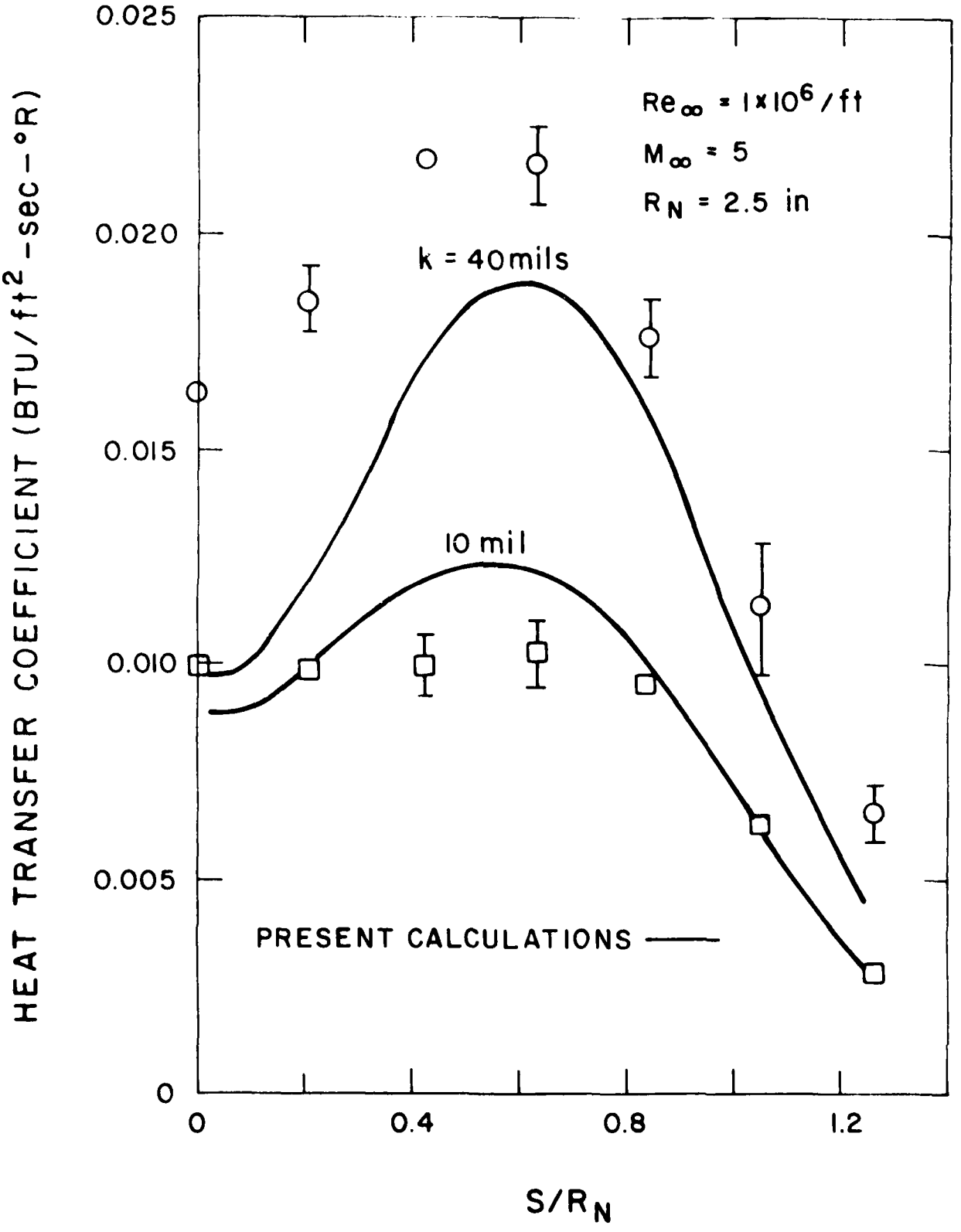

Fig. 9 Comparison With PANT Heat Transfer Data
$Re_\infty = 1 \times 10^6$/ft.

even at the highest Reynolds number; ii) at larger angles ($S/R_N \geq 1$), the computations are inaccurate due to breakdown of the Newtonian pressure distribution employed; iii) significant apparent increases over the theoretical laminar heating rate are observed at the stagnation point ($S/R_N = 0$). The approach taken here yields the laminar result at the stagnation point where there is no production of turbulence since $U_e = 0$ and $\partial U/\partial Y = 0$. We investigated whether a low Reynolds number (Stokes) drag coefficient in R_u (Eq. (13)) plus the corresponding heat transfer term, could increase the heat transfer near (but not at) the stagnation point. The result was negative. In our opinion, the effect of roughness on the stagnation point heat transfer is not presently understood. Random motion of the stagnation point, due perhaps to tunnel disturbances, would increase the heating rate at the mean stagnation point location. However, for the effect to be appreciable, the amplitude of such motion would have to be $\sim 10 - 20^{\circ}$, which seems unlikely. The stagnation point could be unstable to 3-D disturbances of the Goertler type, but the role of roughness in triggering such instabilities has not been demonstrated. We suspect that the stagnation point data of Figs. 6 through 9 are contaminated by heat conduction within the model. A lateral conduction correction was applied in the PANT data reduction, although the thermocouple spacing is much too coarse to resolve the issue.

V. HEAT TRANSFER SCALING LAWS

One particularly useful aspect of this rough wall turbulence model is that the results can be examined to determine the nature of the roughness influence on turbulent boundary layers. One rather conspicuous conclusion is that the Reynolds analogy between friction and heat transfer is <u>not</u> preserved with significant roughness. This result is well known, and derives from the absence of a heat transfer analogy to form drag on the elements. The computations show that the velocity fluctuations increase in proportion to U_τ ($\sqrt{\tau_w/\rho_\infty}$), but the temperature fluctuations are hardly changed by roughness. Since $\tau_w \sim \overline{u'v'}$ and $\dot{q} \sim \overline{v'T'}$ the heat transfer augmentation is the square root of the skin friction augmentation:

$$\frac{St}{St_o} - 1 = \left\{\frac{C_f}{C_{f_o}} - 1\right\}^{1/2} \tag{16}$$

where subscript o denotes smooth wall.

To indicate the appropriate scaling law for the roughness influence, the wall shear is formally given by

$$\tau_w = \mu_w \left(\frac{\partial u}{\partial y}\right)_w + \frac{C_D}{2} \int_0^k \rho U^2 D(y) \frac{1}{\ell^2}\, dy \tag{17}$$

As indicated by Fig. 1, the velocity is significantly altered by roughness. However, for the present purposes we will use the smooth wall law-of-the wall to evaluate the integral in Eq. (17):

$$U = U_{\tau_0} (2.5 \ln y^+ + 5.1) \tag{18}$$

In addition to being in error by up to a factor of two due to roughness, the roughness height can easily extend into the wake region, beyond the validity

of this relation. Neglecting contributions from the laminar sublayer, the lower limit of the integral should be replaced by $y^+ = 10$. For simplicity, we set $D(y) = k$ and $\rho = \rho_w$ in Eq. (17). Inserting Eq. (18) into Eq. (17) and rearranging,

$$\frac{\tau_w}{\tau_{w_0}} = \frac{C_f}{C_{f_0}} = 1 + \frac{\rho_w}{\rho_e} f_1(k^+) \tag{19}$$

$$f_1(k^+) = \frac{C_D}{2} \frac{k^2}{\ell^2} \frac{1}{k^+} \int_{10}^{k^+} (2.5 \ln y^+ + 5.1)^2 \, dy^+$$

$$\sim \frac{C_D}{2} \frac{k^2}{\ell^2} \left\{ 13 \ln k^+ + 6.25 \ln^2 k^+ - 63 \right\} \tag{20}$$

where $k^+ = \rho_w U_\tau k / \mu_w$.

Figure 10 shows the roughness augmentation of skin friction in the format of Eq. (19), according to our computations. Agreement with the incompressible flat plate data was sufficient (cf. Fig. 4) to ensure that the data would plot in a similar manner, but the skin friction was not measured in the sphere tests. The plotted points correspond to fully turbulent conditions; values for $S/R_N < 0.2$ or $Re_\theta < 150$ were omitted. The solid line on the figure is Eq. (20), with $C_D = 0.5$ and $\ell = 5k$. Given the assumptions required to reach Eq. (20), the agreement is surprisingly good. However, a wider range of data should be examined before Eq. (20) would be considered reliable. In particular, the roughness density effect given by k^2/ℓ^2 is probably oversimplified. Changes in roughness density would be expected to yield variations in the actual velocity profile and could lead to a more complex dependence on roughness density.

Figure 11 shows the corresponding plot for the heat transfer augmentation, again based entirely on our computed values. The line

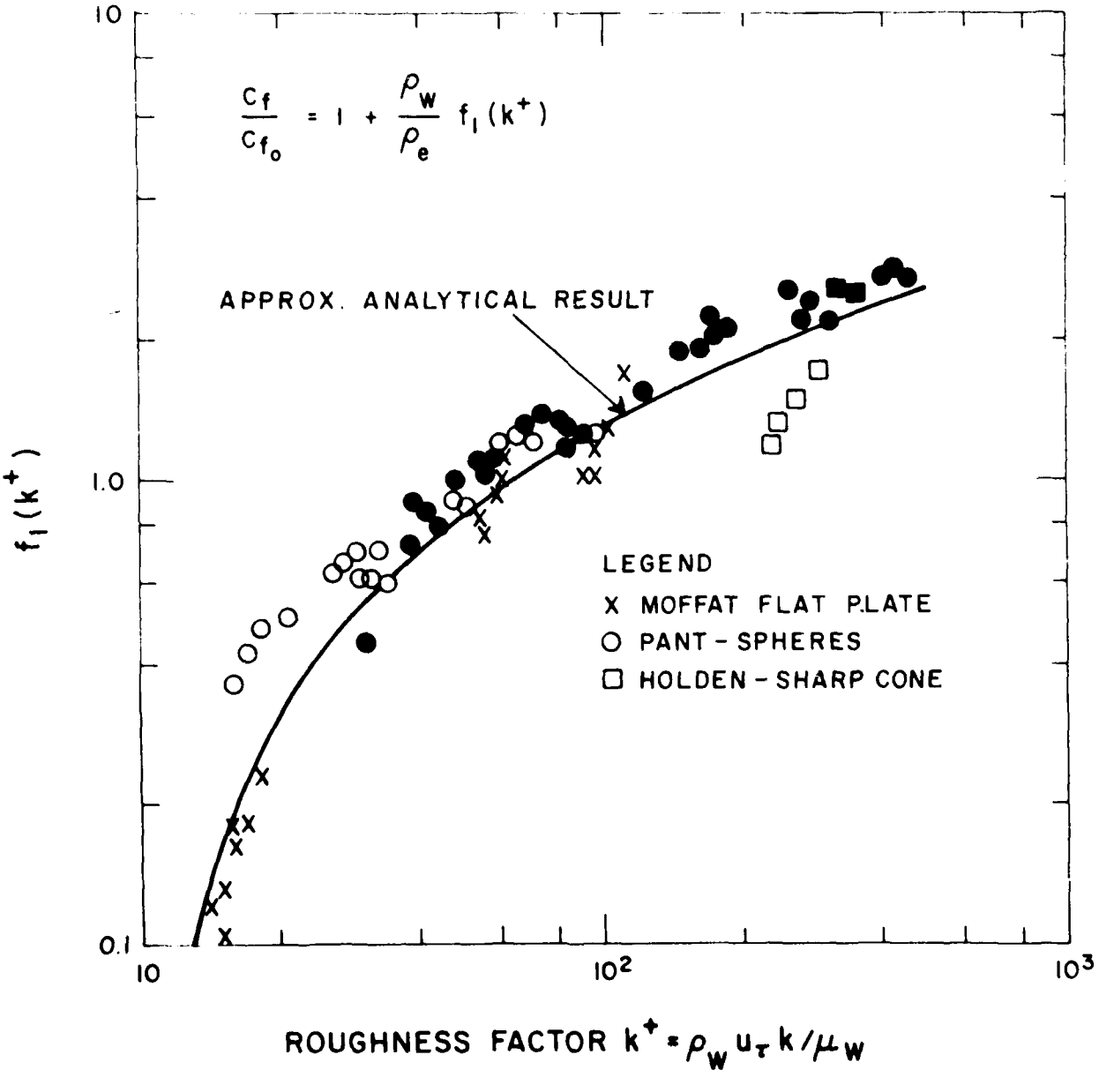

Fig. 10 Roughness Augmentation of Skin Friction
Open symbols: $k/\theta<1$;
Filled symbols: $k/\theta>1$.

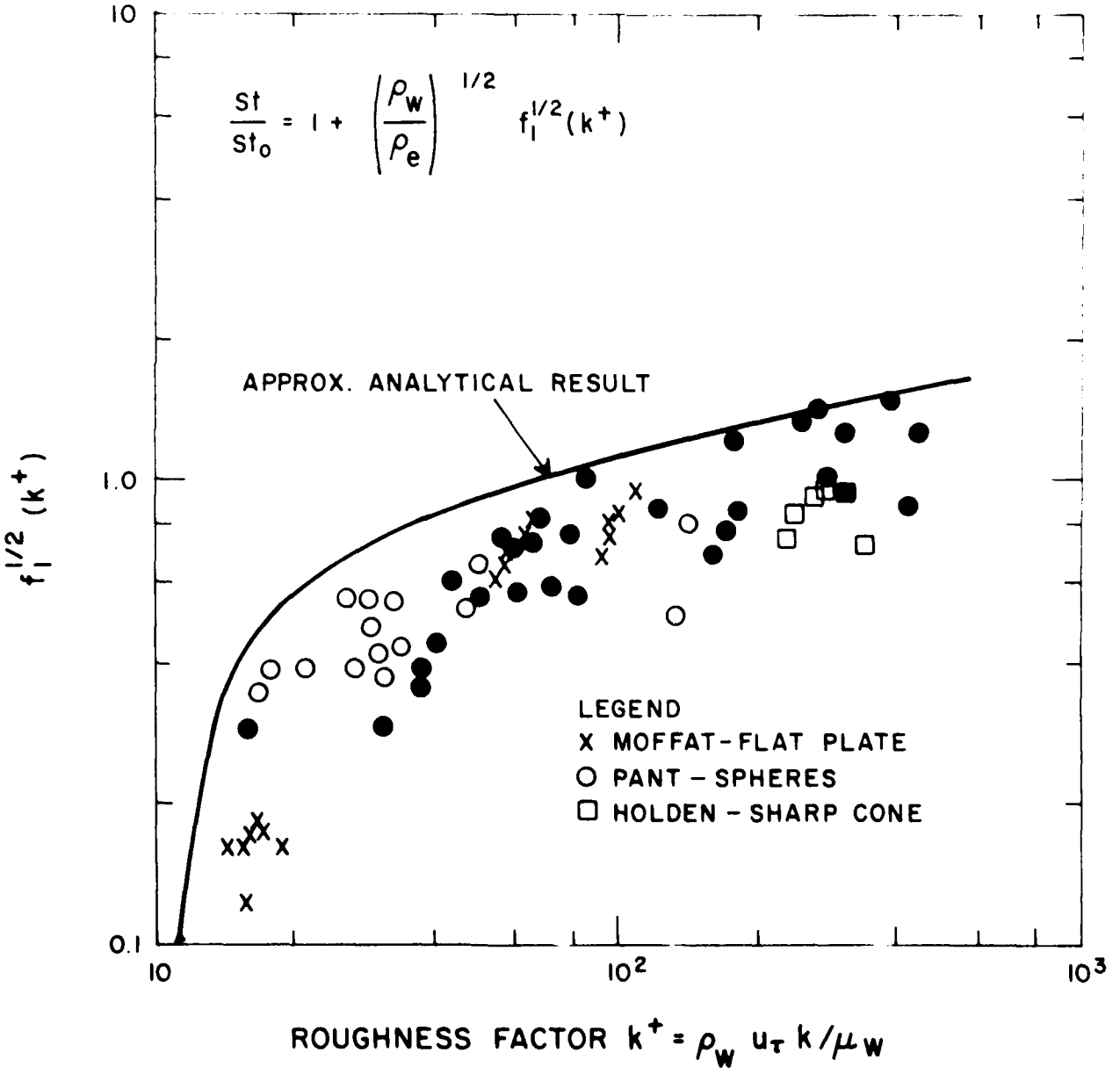

Fig. 11 Roughness Augmentation of Heat Transfer
Open symbols: $k/\theta < 1$;
Filled symbols: $k/\theta > 1$.

corresponds to $f_2 \quad \overline{f_1^{1/2}}$; this manner of applying the square root is only an approximation to Eq. (16), and may be partially responsible for the greater scatter in this figure compared to the previous one. Another reason for the scatter is that Eq. (16) is not strictly correct, in that the temperature fluctuations can be affected somewhat by roughness.

By way of comparison, the skin friction expressions used by Dvorak[3] and Chen[4] are expressed in terms of the displacement thickness rather than wall coordinates:

$$\left(\frac{2}{C_f}\right)^{1/2} \sim A \ln \delta^*/k + f(\text{density}) .$$

The dependence on roughness density has yet to be evaluated with our model; much of the data from which their expression was derived pertain to two-dimensional roughness, which was not considered here.

The correlations of Dahm et al.[6] are closer to the present result, although still with important differences. Their expressions are:

$$\frac{C_f}{C_{f_0}} \quad 1 + 0.5\, f(k/\theta)g(x) \tag{21}$$

$$\frac{St}{St_0} \quad 1 + 0.3\, f(k/\theta)g(x) \tag{22}$$

$f(k/\theta) \quad 1 + 0.09\, k/\theta + 0.53\,(1 - e^{-k/\theta})$

$g(x) \quad x + 1.5\,(1 - e^{-x})\,, \quad x = \log_{10} \frac{k^+}{15.5}$

The function g(x) is quite similar to our $f_1(k^+)$, which is not surprising since it represents a correlation of essentially the same data. The

dependence on k/θ is weak: $f(k/\theta)$ varies by only about 70% between k/θ 1 and 10. We did not consider a dependence on k/θ, although it might arise at large roughness heights that extend beyond the logarithmic velocity region. However, as indicated by the open and filled symbols in Fig. 10, no strong effect is evident. The difference between the factors of 0.5 and 0.3 in Eq. (21) and (22) accomplishes much the same effect as the square root in our result, Eq. (16). One difference that is somewhat significant is the lack of a density dependence in the Dahm correlation; this dependence shows up rather clearly between the subsonic flat plate cases ($\rho_w/\rho_e \tilde{} 1.0$) and the supersonic sphere cases ($\rho_w/\rho_e \tilde{} 0.5$).

VI. FINAL REMARKS

The results presented here are quite encouraging, in that a rather basic model yields results that are in agreement with many observed trends regarding the influence of surface roughness. The assumptions inherent to this model are limited to the basic nature of the flow around the roughness elements, and no approximations have been made regarding profiles of the boundary layer quantities, turbulence levels, or relations between the momentum and energy fluxes.

The present results can undoubtedly be improved and extended. It would be useful to have better data to study on the effects of roughness density and element shape, for distributed roughness. Also, the scaling laws derived in the previous section could be improved if we could better correlate the mean velocity profiles in the presence of roughness. Finally there are other situations that could be examined with the approach presented here, including the combined effect of roughness and mass addition, and the effect of roughness at strongly supersonic or hypersonic edge Mach numbers.

REFERENCES

1. Nikuradse, J., "Strommungsgestze in rauhen Rohren", VDI Forschungsheft, No. 361, SerB, Vol. 4, (1933): English Translation, NACA TM1292, 1950.

2. See Schlichting, H., Boundary Layer Theory, McGraw-Hill, New York, 1968.

3. Dvorak, F. A., "Calculation of Turbulent Boundary Layers on Rough Surfaces in Pressure Gradient", AIAA Journal, Vol. 7, No. 9, Sept. 1969, pp. 1752-1759. Also AIAA J., Vol. 4, No. 11, Nov. 1972, pp. 1447-1451.

4. Chen, K. K., "Compressible Turbulent Boundary-Layer Heat Transfer to Rough Surfaces in Pressure Gradient", AIAA Journal, Vol. 10, No. 5, May 1972, pp. 623-629.

5. Owen, P. R. and Thomson, W. R., "Heat Transfer Across Rough Surfaces", J. of Fluid Mech., Vol. 15, 1963, pp. 321-334.

6. Dihm, F. J. et al., "Passive Nosetip Technology (PANT II) Program, "SAMSO-TR-77-11, Oct. 1976, Acurex Corp., Mountain View, Calif.

7. Healzer, J. M., Moffat, R. J. and Kays, W. M., "The Turbulent Boundary Layer On A Rough, Porous Plate: Experimental Heat Transfer With Uniform Blowing", Thermosciences Division, Department of Mechanical Engineering, Stanford University, Report No. HMT-18, May 1974.

8. Reda, D., "Compressible Turbulent Skin Friction on Rough and Rough/Wavy Walls", AIAA Paper 74-574, Palo Alto, Calif. 1974.

9. Saffman, P. G. and Wilcox, D. C., "Turbulence-Model Predictions for Turbulent Boundary Layers", AIAA Journal, Vol. 12, No. 4, April 1974, pp. 541-546.

10. Finson, M. L., "Hypersonic Wake Aerodynamics at High Reynolds Numbers", AIAA Journal, Vol. III, No. 8, Aug. 1974, pp. 1137-1145.

11. Finson, M. L., et al., "Advanced Reentry Aeromechanics Interim Scientific Report", Report PSI TR-10, AFOSR-TR-74-1785, 1979, Physical Sciences Inc., Woburn, Mass.

12. Finson, M. L., "A Reynolds Stress Model for Boundary Layer Transition with Application to Rough Surfaces", PSI TR-34, 1978, Physical Sciences Inc , Woburn, Mass.

13. Finson, M. L., "On the Application of Second-Order Closure Models to Boundary Layer Transition", AGARD Conference on Laminar-Turbulent Transition, AGARD Conference Proceedings No. 224, Oct. 1977, pp. 23-1 to 23-6.

14. Hanjalic, K. and Launder, B. E., "A Reynolds Stress Model of Turbulence and its Application to Thin Shear Flows", J. Fluid Mech., 52, 609-638 (1972).

15. Launder, B. E., Reece, G. J., and Rodi, W., "Progress in the Development of a Reynolds Stress Turbulence Closure", J. Fluid Mech., 68, 537-566 (1975).

16. Hanjalic, K. and Launder, B. E., "Contribution Toward a Reynolds-Stress Closure for Low-Reynolds-Number Turbulence", J. Fluid Mech., 74, 593-610 (1976).

17. Horstman, C. C. and Owen, F. K., "Turbulent Properties of a Compressible Boundary Layer", AIAA J., 10, 1418-1424 (1972). Also Mikulla, V. and Horstman, C. C , AIAA Paper No. 75 - 119 (1975).

18. Tennekes, H. and Lumley, J. L., "A First Course in Turbulence", MIT Press, Cambridge, Mass., 1972, Section 4.2.

19. Moffat, R. J. and Kays, W. M., "The Turbulent Boundary Layer on a Porous Plate: Experimental Heat Transfer with Uniform Blowing and Suction", Report No. H MT-1, Thermosciences Division, Dept. of Mech. Eng., Stanford University, 1967.

20. Pimenta, M. M., "The Turbulent Boundary Layer: An Experimental Study of the Transport of Momentum and Heat with the Effect of Roughness", Ph. D. Dissertation, Dept. of Mech. Eng., Stanford University, 1975.

21. Jackson, M. D. and Baker, D. L., "Passive Nosetip Technology (PANT) Program Interim Report", Vol. III, Part I, SAMSO-TR-74-86, Jan. 1974, Acurex Corp., Mountain View, Calif.